

Introduction

Cloud Cluster

Definition

1. The oval-shaped cloud mass region of T_B (equivalent black-body temperature) lower than -50° is about or larger than 100 km in diameter
2. Horizontal gradient of T_B is large near the rim of the cloud mass (at least a part of the rim)

- Among four major types of Heavy Precipitation Systems (HPSs) over the Korean peninsula, cloud clusters occur most frequently and produce large amount of rainfall over broad area

Table 1. Frequency of heavy precipitation systems for each type of precipitation system for 2000-2006.

Type	Isolated thunderstorm (IS)	Convection band (CB)	Cloud cluster (CC)	Signal line (SL)	Not defined	Total
June	4	2	11	2	3	22
July	3	17	25	3	4	52
August	6	12	17	3	1	39
Total	13	31	53	8	8	113
	(11.5)	(27.4)	(46.9)	(7.1)	(7.1)	(100%)

(Lee and Kim, 2007)

Environment

1. In the eastern part of low-level trough (or cyclone) or along the activated monsoon front trailing behind a trough (or cyclone)
2. Over a stationary monsoon front far from the trough

Movement

Generally move along the front or move together with the pressure system in which they are embedded

Objective

- To investigate the structure and evolution of cloud cluster occurred on 2 July 2008 by using various observational data and numerical simulation.

Observational analysis

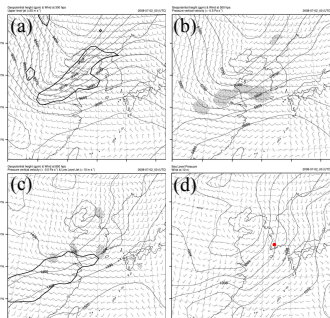


Fig. 1. Synoptic analysis at 00 UTC 2 July. (a) 300 hPa, (b) 500 hPa, (c) 850 hPa and (d) surface. The red circle in (d) indicates Gwangju.

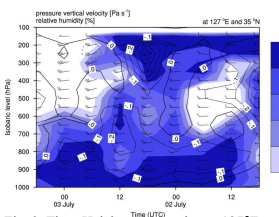


Fig. 2. Time-Height cross section at 127°E and 35°N.

- At 00 UTC 2 July, a 300 hPa jet streak associated with the upper level trough over the north-eastern China extended from eastern China to Northern Korea
- Upward motion existed over east China and the south of Yellow sea in advance of 500 hPa shortwave trough
- 850 hPa upward motion appeared in front of the west-southwesterly low-level jet (LLJ)
- Surface low-pressure center strengthened over the northwest of the Korean peninsula

- High relative humidity appeared in the layer between 1000 and 850 hPa
- After 06 UTC, 900 hPa wind changed from southerly to west-southwesterly and wind speed began to increase
- After 06 UTC, dry region (RH<80%) appeared at 850 hPa

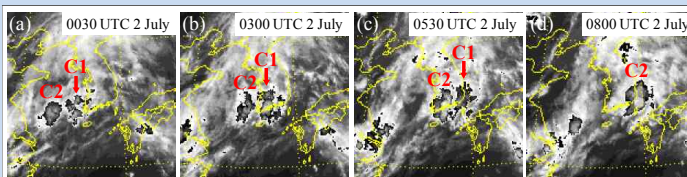


Fig. 3. MTSAT enhanced IR imagery for (a) 0030 UTC, (b) 0300 UTC, (c) 0530 UTC, and (d) 0800 UTC 2 July.

- 2 July 2008 case consisted of two precipitation systems (C1 and C2)
- Two precipitation systems migrated through southern Korean peninsula and produced rainfall over broad area

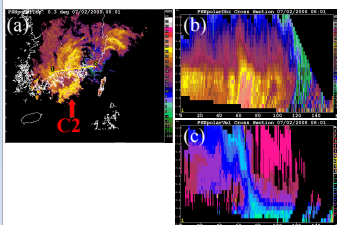


Fig. 4. (a) Pusan (PSN) radar reflectivity image for 06 UTC 2 July. Cross section of (b) Reflectivity and (c) radial velocity along a line in (a).

- Configurable Interactive Data Display System (CIDD) is available for high resolution radar data analysis
- C2 shows a **bow-shape echo**
- Strong mid-level wind appeared at the rear of convection

Numerical simulation

Weather Research and Forecasting (WRF) Model V3.1

Table 2. Model configuration.

	D01	D02	D03
Horizontal grid spacing	30 km (169×160)	10 km (250×202)	3.3 km (232×202)
Vertical layers	41 layers (model top : 50 hPa)		
Cumulus	Betts-Miller-Janjic scheme No Cumulus		
Microphysics	WSM 6-class graupel scheme		
Longwave radiation	RRTM scheme		
Shortwave radiation	Dudhia scheme		
PBL	Mellor-Yamada-Janjic TKE scheme		
Surface	Unified Noah land-surface model		
IC & BC	NCEP FNL Output of D1 Output of D2		

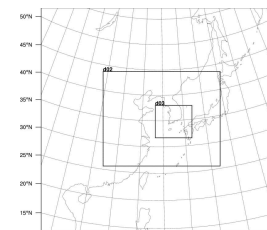


Fig. 5. The three two-way nested domains for the numerical simulation.

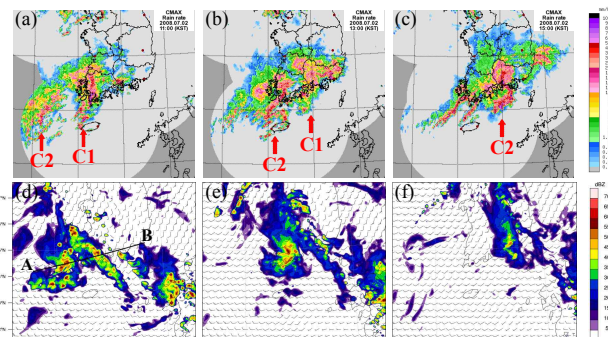


Fig. 6. Composited maximum radar reflectivity for (a) 02 UTC, (b) 04 UTC, and (c) 06 UTC 2 July. Simulated maximum radar reflectivity and wind field at 925 hPa for (d) 02 UTC, (e) 04 UTC, and (f) 06 UTC 2 July.

- The simulated maximum reflectivity fields for C2 coincide with the observed radar reflectivity
- Simulated C2 dissipates over inland while observed C2 sustain its shape and intensity

Moisture Flux Convergence (MFC)

$$MFC = -\nabla \cdot (q \mathbf{V}_h) = \underbrace{-\mathbf{V}_h \cdot \nabla q}_{\text{advection term}} - \underbrace{q \nabla \cdot \mathbf{V}_h}_{\text{convergence term}}$$

(Banacos and Schultz, 2005)

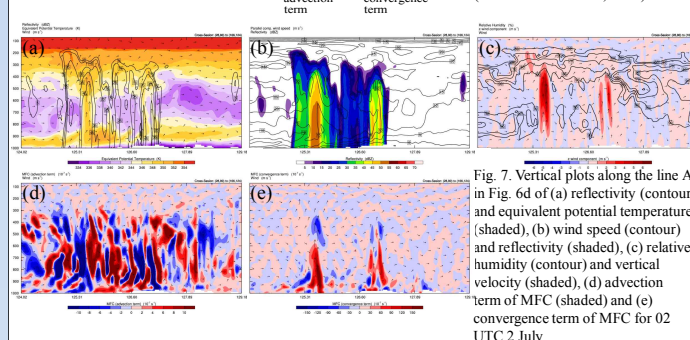


Fig. 7. Vertical plots along the line AB in Fig. 6d of (a) reflectivity (contour) and equivalent potential temperature (shaded), (b) wind speed (contour) and reflectivity (shaded), (c) relative humidity (contour) and vertical velocity (shaded), (d) advection term of MFC (shaded) and (e) convergence term of MFC for 02 UTC 2 July.

- High θ_e air is supplied toward convective region by strong west-southwesterly in the layer between 1000 and 900 hPa
- Strong horizontal gradient of parallel component wind speed appear in the layer between 850 and 600 hPa at the convective region
- Dry region appear in the layer between 900 and 700 hPa at the rear of convection
- Large value of convergence term of MFC coincide well with upward motion

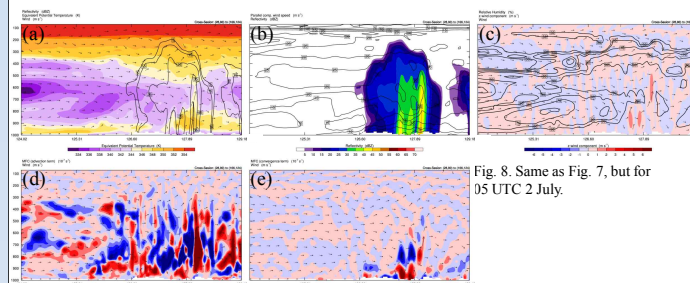


Fig. 8. Same as Fig. 7, but for 05 UTC 2 July.

- Inflow of high θ_e air is cut off as dry and cold mid-level air reached to surface at the rear of convection
- Strong MFC still existed in the layer between 1000 and 900 hPa, but strong moisture flux divergence appeared just above strong MFC

Summary & Future Plan

- Existence of warm and moist air and its strong convergence in the low-level play an important role in sustaining the active convection
- The formation of bow-shape echo might be affected by low θ_e air in the mid-level at the rear of convection
- It needs to be identified explicitly what is the role of the dry region in the mid-level for the formation of bow-shape echo
- It also has to be studied what relationship exists between the circulation induced by active convection and the dry region in the mid-level at the rear of convection

Acknowledgement

- This work has funded by the Korea Meteorological Administration Research and Development Program under Grant CATER 2006-2304.